Mice expressing a dominant-negative Ret mutation phenocopy human Hirschsprung disease and delineate a direct role of Ret in spermatogenesis

Sanjay Jain[1], Cathy K. Naughton[2], Mao Yang[1], Amy Strickland[2], Kiran Vij[1], Mario Encinas[3], Judy Golden[3], Akshay Gupta[2], Robert Heuckeroth[4], Eugene M. Johnson, Jr[3] and Jeffrey Milbrandt[1,*]

[1]Department of Pathology and Immunology, Washington University School of Medicine, 660 South Euclid Avenue, St Louis, MO 63110, USA
[2]Department of Urologic Surgery, Washington University School of Medicine, 660 South Euclid Avenue, St Louis, MO 63110, USA
[3]Department of Molecular Biology and Pharmacology, Washington University School of Medicine, 660 South Euclid Avenue, St Louis, MO 63110, USA
[4]Department of Pediatrics, Washington University School of Medicine, 660 South Euclid Avenue, St Louis, MO 63110, USA
*Author for correspondence (e-mail: jeff@pathbox.wustl.edu)

Accepted 25 August 2004

Development 131, 5503-5513
Published by The Company of Biologists 2004
doi:10.1242/dev.01421

Summary

The Ret receptor tyrosine kinase mediates physiological signals of glial cell line-derived neurotrophic factor (GDNF) family ligands (GFLs) and is essential for postnatal survival in mice. It is implicated in a number of human diseases and developmental abnormalities. Here, we describe our analyses of mice expressing a Ret mutant (*Ret*DN) with diminished kinase activity that inhibits wild-type Ret activity, including its activation of AKT. All $Ret^{DN/+}$ mice died by 1 month of age and had distal intestinal aganglionosis reminiscent of Hirschsprung disease (HSCR) in humans. The $Ret^{DN/+}$ proximal small intestine also had severe hypoganglionosis and reduction in nerve fiber density, suggesting a potential mechanism for the continued gastric dysmotility in postsurgical HSCR patients. Unlike *Ret*-null mice, which have abnormalities in the parasympathetic and sympathetic nervous systems, the $Ret^{DN/+}$ mice only had defects in the parasympathetic nervous system. A small proportion of $Ret^{DN/+}$ mice had renal agenesis, and the remainder had hypoplastic kidneys and developed tubulocystic abnormalities postnatally. Postnatal analyses of the testes revealed a decreased number of germ cells, degenerating seminiferous tubules, maturation arrest and apoptosis, indicating a crucial role for Ret in early spermatogenesis.

Key words: Ret, GDNF, Hirschsprung disease, Spermatogenesis

Introduction

Mutations in *RET*, a transmembrane receptor tyrosine kinase (RTK), act in a dominant manner and cause multiple human diseases (Ponder and Smith, 1996). For example, inactivating *RET* mutations are a common cause of Hirschsprung disease (HSCR), or distal intestinal aganglionosis, a disorder that affects 1 in 5000 infants. By contrast, activating *RET* mutations lead to human multiple endocrine neoplasia (MEN) syndromes 2A and 2B. Other diseases, such as Parkinson's and motor neuron disease, involve neuronal populations that respond to Ret ligands, glial cell line-derived neurotrophic factor (GDNF) family ligands (GFLs). Thus, it is thought that increasing Ret activation through administration of these factors may be useful in treating these patients (Airaksinen and Saarma, 2002).

Numerous studies have demonstrated that Ret activation is essential for the proper embryologic development of the kidneys, and the autonomic and enteric nervous systems (ENS) (Enomoto et al., 2001; Enomoto et al., 2000; Schuchardt et al., 1994). From the analyses of mice deficient in neurturin (NRTN) or GFRα2, it has been suggested that Ret is also important for the postnatal maintenance of the enteric and parasympathetic nervous systems, while a role in spermatogenesis has been suggested following the analysis of mice that overexpress GDNF in the testes (Gianino et al., 2003; Heuckeroth et al., 1999; Meng et al., 2000; Rossi et al., 1999). Unfortunately, the perinatal lethality of Ret-null animals has made it impossible to study the postnatal roles of Ret, and to develop animal models that mimic Ret-related human diseases. This has hindered the molecular understanding of these diseases, and the subsequent development and testing of novel treatment strategies.

Ret signaling is mediated by the binding of the GFLs [GDNF, neurturin (NRTN), artemin (ARTN) and persephin (PSPN)] with their cognate glycophosphatidylinositol (GPI)-anchored GFRα1-4 co-receptor, and their subsequent interaction with the Ret extracellular domain (Baloh et al., 2000). These interactions result in functional GFL-GFRα-Ret complexes and the autophosphorylation of key Ret tyrosine residues that harbor consensus sequences for adaptor proteins. Recruitment of these adaptor proteins to phosphorylated Ret tyrosine residues activates multiple signaling pathways, including the mitogen-activated protein kinase (MAPK) and the phosphoinositide 3-kinase (PI3K)-AKT pathways that regulate cell survival, proliferation, migration and axonal

outgrowth. The perturbation of these key processes leads to the various abnormalities observed in Ret-null mice (Airaksinen and Saarma, 2002), but the specific regions of Ret that regulate these cellular processes, and are associated with the proper development and function of the nervous and urinary systems, are unknown.

To better understand the roles of the key signaling domains of Ret in mediating its diverse biological effects, we generated a mouse expressing a Ret protein (RetDN) with mutations in the Ret cytoplasmic tail. Mice harboring one copy of the RetDN allele (*Ret*$^{DN/+}$) exhibit long-segment intestinal aganglionosis reminiscent of human patients with HSCR, where aganglionosis due to *RET* mutations manifests in the heterozygous state, and is typically restricted to the colon and/or distal small intestine. The intestinal phenotype is distinct from previous Ret loss-of-function murine models where the loss of one allele does not cause significant morphologic abnormalities of the ENS (Gianino et al., 2003), whereas Ret-null homozygotes show a complete loss of ganglion cells in the entire intestine (Schuchardt et al., 1994). These studies also highlight the differing requirements for Ret signaling in the peripheral nervous system, as deficits are found in both branches of the autonomic nervous system in Ret-null mice, but *Ret*$^{DN/+}$ mice have defects only in the parasympathetic nervous system. The postnatal survival of the *Ret*$^{DN/+}$ mice allowed us to clearly demonstrate the postnatal importance of Ret signaling for the maintenance of the ENS and parasympathetic nervous systems, and the requirement for Ret during the first wave of spermatogenesis.

Materials and methods

Generation of various *Ret* knockin mice

Human *RET* cDNA constructs were homologously recombined into the first coding exon of the *Ret* gene in a manner that disrupts synthesis of the endogenous mouse Ret. We previously used this targeting strategy to generate Ret-null mice (*Ret*$^{TGM/TGM}$) (Enomoto et al., 2001). In these studies, the tauEGFP-myc (TGM) reporter gene was replaced with human *RET* cDNAs encoding either the RET9 isoform (*Ret*9 allele) or a RET9 mutant (*Ret*DN allele) that contains mutations at L985P and Y1062F (see Fig. 1A,B). Mutant mice were successfully generated using standard methods (Enomoto et al., 2001). Germline transmission of the recombined alleles was confirmed by Southern blotting (Fig. 1C). All experiments were performed on mice with a mixed genetic background (129/SvJ:C57BL/6; F1-F4 generation). Routine genotyping was performed using polymerase chain reaction (PCR). The mouse wild-type *Ret* allele (449 bp PCR product) was identified with primers from the 5′UTR, P6855 (5′-CAGCGCAGGTCTCTCATCAGTACCGCA-3′), and from the first intron, P4828 (5′-CAGCTACCCGCAGCGA-CCCGGTTC-3′). The introduced human *Ret*9 or *Ret*DN alleles (310 bp PCR product) were identified with P6855 and a reverse primer from the human RET coding region (5′-AGCATCCCTCGAGA-AGTAGAGG-3′) (94°C, 45 seconds; 60°C, 45 seconds; 72°C, 45 seconds; 35 cycles). Excision of the neomycin resistance cassette by breeding to β-actin Cre transgenic mice (Meyers et al., 1998) for removal of the floxed neomycin resistance marker was confirmed using PCR with a primer from the 3′ UTR of the human *RET* cDNA, P4665 (5′-TGAATGCAATTGTTGTTGTTAACT-3′), and from the endogenous mouse *Ret* locus (P4828). All of the phenotypes described were observed in mice derived from two independent *Ret*$^{DNneo/+}$ ES cell clones.

Tissue RNA analysis

Total RNA was isolated from brain, spinal cord, dorsal root ganglion (DRG) and eye and analyzed by RT-PCR as previously described (Svaren et al., 2000). Total *Ret* transcripts (representing endogenous mouse and the inserted human sequences) were identified using RT-PCR with a forward primer (nucleotide 2908; 5′-GATGG-AGAGGCCAGACAACTGCA-3′) and a reverse primer (nucleotide 3175; 5′-TTTCAATCCATGTGGAAGGGAGG-3′) (all nucleotide designations are relative to the human *RET* coding region). Human *RET* mRNA was identified by RT-PCR with P3366 (nucleotide 2978; 5′-ACAAAAGGCCGGTGTTTGCGGACA-3′) and P9322 (reverse primer from 3′UTR; 5′-CAAGTTAACAACAACAATTGCATTC-3′). Transcripts corresponding to the Ret-null allele were identified as previously described (Enomoto et al., 2001).

Histopathological analysis and immunohistochemistry

Mouse tissues were processed for histological analysis as previously described (Enomoto et al., 2000). Catecholaminergic neurons were visualized with diaminobenzidine by means of tyrosine hydroxylase (TH) immunohistochemistry (rabbit polyclonal antibody, Chemicon, 1:200) in whole-mount (for sympathetic neurons) or in 60-μm unmounted floating sections (for midbrain dopaminergic neurons) (Enomoto et al., 2001). The innervation of intraorbital harderian glands was examined with PGP9.5 (rabbit polyclonal antibody, Biogenesis, 1:400) and Alexa488-conjugated anti-rabbit immunoglobulin secondary antibody (1:250). The small nociceptive DRG sensory neurons were visualized with $P2X_3$ (guinea pig polyclonal antibody, Chemicon, 1:800) and Cy3-conjugated anti-guinea pig secondary antibody (1:400). Germ cells were identified with germ-cell nuclear antigen (GCNA) immunohistochemistry (rabbit polyclonal antibody, 1:500; gift from G. Enders, University of Kansas Medical Center, Kansas, USA). In vivo 5-bromo-2-deoxyuridine (BrdU) labeling (200 mg/kg, Sigma) and anti-BrdU immunohistochemistry (1:200) were used for proliferation studies (Enomoto et al., 2001). Cell death was analyzed using TUNEL assay (Boehringer Mannheim) (Enomoto et al., 2000). Quantitative analyses were performed with SigmaPlot software (SPSS), and statistical significance was determined by Student's *t*-test. For all studies, the sample size was three or more for each genotype, unless otherwise stated.

Enteric neuron studies

Intestinal aganglionosis was evaluated by whole-mount acetylcholinesterase (AChE) staining on dissected intestines of newborn to 3-week-old mice (Enomoto et al., 1998). Quantitative analysis of neuron number and myenteric plexus fibers was performed as described previously (Gianino et al., 2003). The myenteric and submucosal neuron numbers were determined using 20 randomly selected Cuprolinic Blue-stained intestine regions and 10 randomly selected AChE-stained intestine regions, respectively (0.25 mm^2/counting grid area×10-20 areas/mouse×3 mice of each genotype). Myenteric plexus fiber density was determined from 10 randomly selected fields/mouse (30 regions per genotype), by counting the number of fibers crossing the left and top edge of a 0.25-mm^2 grid.

Parasympathetic neuron studies

The number of sphenopalatine ganglion neurons was determined from thionin-stained, paraffin-embedded coronal head sections (6 μm) of newborn mice. The entire ganglion was sectioned, and neurons with distinct nucleoli were counted at 60-μm intervals (at least 3 animals, 6 ganglia, from each genotype) (Enomoto et al., 2000). Cell size analysis was performed on dissected postnatal sphenopalatine ganglia (P21). Thirty neurons were used from each animal for area determination with image analysis software (http://www.chemie.uni-marburg.de/~becker/image.html).

Spinal motor neurons cell counts

Spinal cords from 3-week-old animals were paraffin embedded, sectioned (12 μm), stained with thionin, and the number of motor neurons in the entire lumbar enlargement, L1-L6 (counted at 120-μm intervals) was determined. Cells with large cell bodies, granular cytoplasm and prominent nucleoli were counted (Clarke and Oppenheim, 1995).

Analysis of the genitourinary system

To determine relative nephron number, we serially sectioned newborn kidneys in their entirety and counted glomeruli every 120 μm (Majumdar et al., 2003). For spermatogenesis studies, testes were harvested at the indicated time points for either histological or ploidy studies. For quantification, seminiferous tubules appearing in cross section were used. Germ cell number (GCNA immunohistochemistry), apoptosis (TUNEL-assay positive), or proliferation (BrdU incorporation) in $Ret^{DN/+}$ and wild-type mice were determined from 100 random seminiferous tubules of each animal.

Flow cytometry

For ploidy studies, testes were decapsulated and triturated into a single cell suspension in Hank's balanced salt solution that contained propidium iodide (50 μg/ml), citric acid (1 mg/ml), and Nonidet P40 (0.3%) for 30 minutes. Ten thousand cells were analyzed for their DNA content on a FACScan (Becton Dickinson) with FlowJo software (Tree Star, Version 4.3).

In vitro experiments

The human *Ret* cDNAs used for these studies include Ret9, Ret9(Y1062F), Ret9(K758M), Ret9-FLAG, RetDN-HA and Ret9(L985P, Y1062F), also called RetDN, and either have been previously described (Tsui-Pierchala et al., 2002) or were generated in the pcDNA3.1 vector (Invitrogen) using standard methods. Lentiviruses that harbor the different Ret cDNAs in pFCIV-1 (Crowder et al., 2004) were prepared by standard methods (Lois et al., 2002; Naldini et al., 1996). Cell populations expressing equivalent levels of each of the Ret proteins in the infected CHP126, 293T or Neuro2Aα1 cell lines were obtained as described (Crowder et al., 2004). For ligand stimulation, cells were grown in low serum (0.5%) for 4 hours and then exposed to GDNF (25 ng/ml) for 10 minutes before harvest.

Western blot and immunoprecipitation of cell extracts from cell lines or primary superior cervical ganglion (SCG) cultures were performed as described previously (Tsui-Pierchala et al., 2002). The primary antibodies (1:1000) were as follows: rabbit anti-panRet and anti-pY1062 (Tsui-Pierchala et al., 2002), rabbit anti-AKT and anti-pAKT (Cell Signaling Technologies), rabbit anti-pMAPK (New England Biolabs), rabbit anti-pY20 (BD Biosciences), and rabbit anti-FLAG and rabbit anti-Actin (Sigma, St Louis). The secondary peroxidase-conjugated anti-rabbit antibodies (Jackson Immuno) were used at 1:10,000. Signals were detected with chemiluminescence with the Super Signal West Dura kit (Pierce) on an EPI CHEM II Darkroom instrument (UVP). The normalization and analysis for ligand-dependent phosphorylation of AKT was performed using LabWorks Image Acquisition and Analysis software (UVP). Phospho-AKT levels were normalized to the amount of total AKT in the cells.

Results

Growth retardation and postnatal death in $Ret^{DN/+}$ mice

Ret-null mice have developmental defects of the peripheral nervous system and kidneys (Enomoto et al., 2001; Enomoto et al., 2000; Schuchardt et al., 1994), but the roles of individual domains or residues within Ret that are required for normal development have not been identified. To identify specific intracellular signaling pathways that are essential for Ret biological activity, we introduced a human *RET9* cDNA, either wild type or with a mutation in the key docking tyrosine residue (Y1062F), into the *Ret* locus (Fig. 1A) (Enomoto et al., 2001). Among the two major RET isoforms, RET9 and RET51, we chose to study the signaling properties of the mutant RET9 isoform because wild-type RET9 is sufficient and necessary for normal development in mice (de Graaff et al., 2001). Further analysis revealed an additional inadvertent point mutation (L985P) at the end of the kinase domain in the RET9(Y1062F) targeting construct (Fig. 1B; data not shown). Mice containing wild-type human *RET9* (*Ret*9) or mutant human RET9(L985P, Y1062F) (also referred to as *Ret*DN) cDNA at the *Ret* locus were successfully generated, and Cre-mediated excision of the neomycin resistance cassette was confirmed (Fig. 1C; data not shown).

The mutant *Ret*DN allele was inactive when the neomycin resistance cassette was present, but was activated when this cassette was excised by mating with β-actin Cre animals. Interestingly, all of the F1 hemizygous *Ret*DN mice produced in this manner displayed growth retardation and died by 4 weeks of age (Fig. 1D,E). This was surprising as one wild-type mouse *Ret* allele ($Ret^{-/+}$ or $Ret^{TGM/+}$) is sufficient for viability, fertility, and proper development of all known Ret-dependent tissues (Enomoto et al., 2001; Gianino et al., 2003; Schuchardt et al., 1994). Furthermore, hemizygous mice expressing wild-type human RET9 ($Ret^{9/+}$) were viable and fertile with no developmental defects (Fig. 1B,C; data not shown), confirming that expression of the mutant *Ret*DN allele is responsible for the observed phenotype. Because of the dominant effect of this Ret mutant, we refer to this protein as RetDN and to mice harboring this mutant allele as $Ret^{DN/+}$. We detected mRNAs specific to the recombined *Ret*9 or *Ret*DN alleles by RT-PCR at several sites of Ret expression (e.g. brain, spinal cord and eyes; Fig. 1F; data not shown). The early lethality of $Ret^{DN/+}$ mice made the propagation of this line difficult. However, we were able to maintain this line by taking advantage of the diminished expression of the mutant *Ret*DN allele caused by retention of the neomycin resistance cassette ($Ret^{DNneo/+}$) (Fig. 1B,C,F) (Barrow and Capecchi, 1996; Rijli et al., 1994; Schuchardt et al., 1994). The $Ret^{DNneo/+}$ mice had no overt abnormalities (see below, and data not shown).

Long-segment distal intestinal aganglionosis in $Ret^{DN/+}$ mice

$Ret^{DN/+}$ mice developed increasing abdominal distension with age. Because *Ret* null mice have extensive intestinal aganglionosis (i.e. no enteric neurons in the small bowel or colon) and patients with heterozygous-inactivating *RET* mutations have HSCR, we postulated that failure to thrive in $Ret^{DN/+}$ mice could result from defective ENS development. Indeed, gross examination of the gastrointestinal system showed narrowing of the distal bowel, preceded by dilation of the proximal colon or ileum typical of gut morphology in patients with HSCR (Fig. 2A).

To determine whether the abnormal intestines in $Ret^{DN/+}$ mice were due to ENS defects, we examined the myenteric and submucosal plexus using whole-mount staining methods (Fig. 2B). The $Ret^{DN/+}$ mice had intestinal aganglionosis of varying severity that involved the distal colon and often extended past

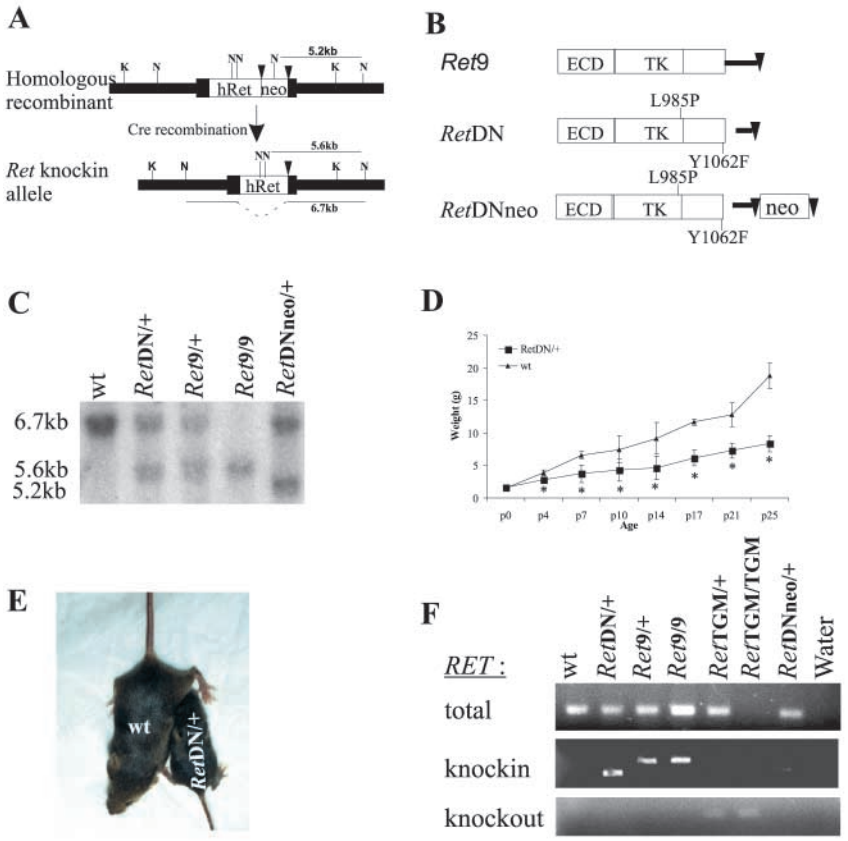

Fig. 1. *Ret*$^{DN/+}$ mice fail to thrive. (A) Mutant or wild-type human *RET9* cDNA was introduced into exon 1 (black box) of the mouse *Ret* locus (black triangles, *loxP* sites). The restriction sites (K, *Kpn*I; N, *Nco*I) and length of the expected fragments in Southern blots are indicated. (B) Schematic of Ret knocked-in alleles. Open box, RET9 cDNA; black line, SV40 3′UTR; ECD, extracellular domain; TK, tyrosine kinase domain; triangle, loxP sites; L985P and Y1062F, RET mutations in the DN allele. (C) Southern blot analysis confirmed successful generation of Ret mutant mouse lines. (D) Growth curves of *Ret*$^{DN/+}$ and wild-type (wt) littermates at indicated postnatal time points (n=3 for each time point; *=P<0.01; error bars, mean±s.d.). (E) Photograph showing the typical size difference between 3-week-old *Ret*$^{DN/+}$ and wild-type littermates. (F) Expression of Ret mutant alleles in mouse brain RNA (P0) by RT-PCR. Total, endogenous mouse and knocked-in human RET; knockin, mice harboring the indicated human *RET* cDNA (Ret9 or RetDN) in the *Ret* locus generate a knockin-specific product; knockout, Ret^{TGM} mice where the *ret* locus is inactivated with the TGM allele. Note that retention of the neomycin resistance gene (*Ret*$^{DNneo/+}$) results in a marked reduction in expression of the knocked-in RetDN allele. wt, wild type. cDNAs knocked-in in the *ret* locus: *Ret*DN, mutant human *RET9* (L985P, Y1062F); *Ret*9, human wild-type *RET9*; *Ret*TGM, tauEGFP-myc; *Ret*DNneo, retained neomycin resistance gene in *Ret*DN allele. '+' denotes one copy of the endogenous mouse allele.

the ileocecal junction into the small intestine (Fig. 2B,C). Regions of aganglionosis were confirmed with routine histological examinations, and by AChE and nicotinamide adenine dinucleotide phosphate (NADPH) diaphorase whole-mount histochemical methods to evaluate non-overlapping populations of enteric neurons (Fig. 2B; data not shown). The extent of distal intestinal aganglionosis was reminiscent of long-segment HSCR, and explained the grossly narrowed distal bowel, poor growth and early death of *Ret*$^{DN/+}$ mice. The severity of this anomaly was accentuated by the observation that some *Ret*$^{DN/+}$ animals died from bowel perforation before they could be analyzed (S.J., unpublished). Interestingly, the macroscopic transition zone (change from narrow caliber to dilated caliber) did not correlate perfectly with the microscopic extent of aganglionosis (histochemically identified change from aganglionic to innervated bowel) in these animals. Instead, parts of dilated bowel (5-50% of distal dilated bowel) were also aganglionic in *Ret*$^{DN/+}$ mice. This discrepancy between the macroscopic and microscopic transition zones in the *Ret*$^{DN/+}$ mice is a phenocopy of the long-segment intestinal aganglionosis seen in HSCR patients with *RET* mutations (Shimotake et al., 2003). All of the other mice examined (*Ret*$^{9/+}$, *Ret*$^{TGM/+}$, *Ret*$^{DNneo/+}$, wild type) had normal ENS structure (Fig. 2C).

To determine whether the ENS anomalies observed in *Ret*$^{DN/+}$ mice were restricted to the distal bowel, we also performed quantitative analysis of the ENS on whole-mount preparations of the proximal duodenum in wild-type and mutant mice. Although the proximal bowel has generally been assumed (with little data) to be 'normal' in patients with HSCR, *Ret*$^{DN/+}$ mice had a remarkable reduction in both neuron number and neuronal fiber density in the proximal small bowel (Fig. 2B,D). These reductions are reminiscent of ENS deficits that appear in GDNF (decreased neuron number) or NRTN (decreased fiber density) deficient mice, indicating that *Ret*$^{DN/+}$ mice have a combination of deficits resulting from an overall reduction in GFL-mediated Ret activation (Gianino et al., 2003; Heuckeroth et al., 1999; Rossi et al., 1999).

Defects in the parasympathetic, but not sympathetic, nervous system in *Ret*$^{DN/+}$ mice

Among the parasympathetic cranial ganglia, the sphenopalatine ganglia (SPG) are the most severely affected in *GDNF*- and *Ret*-null mice. In these mutant mice, the SPG have a marked reduction or absence of neurons that can be primarily attributed to a reduction in neuronal precursor proliferation (Enomoto et al., 2000). We observed a 50% decrease in neuron number in newborn *Ret*$^{DN/+}$ mice, when compared with controls (wild type, *Ret*$^{9/+}$, *Ret*$^{TGM/+}$) (Fig. 3A). While GDNF-mediated Ret activation is crucial for formation of SPG neurons, NRTN and GFRα2 are necessary for SPG trophic maintenance and innervation of the intraorbital harderian glands (Heuckeroth et al., 1999; Rossi et al., 1999). The postnatal survival of *Ret*$^{DN/+}$ mice allowed us to determine whether the SPG neurons that were generated are affected by the decreased Ret activity. We found that *Ret*$^{DN/+}$ SPG neurons are smaller in size than those of wild-type littermates at 3 weeks of age (Fig. 3A). Additionally, PGP9.5 immunostaining revealed abnormal innervation of the harderian glands by *Ret*$^{DN/+}$ SPG neurons (Fig. 3A). Thus, *Ret*$^{DN/+}$ mice have deficits in SPG neuron number, size and target innervation that are a combination of the defects observed in *GDNF*- and

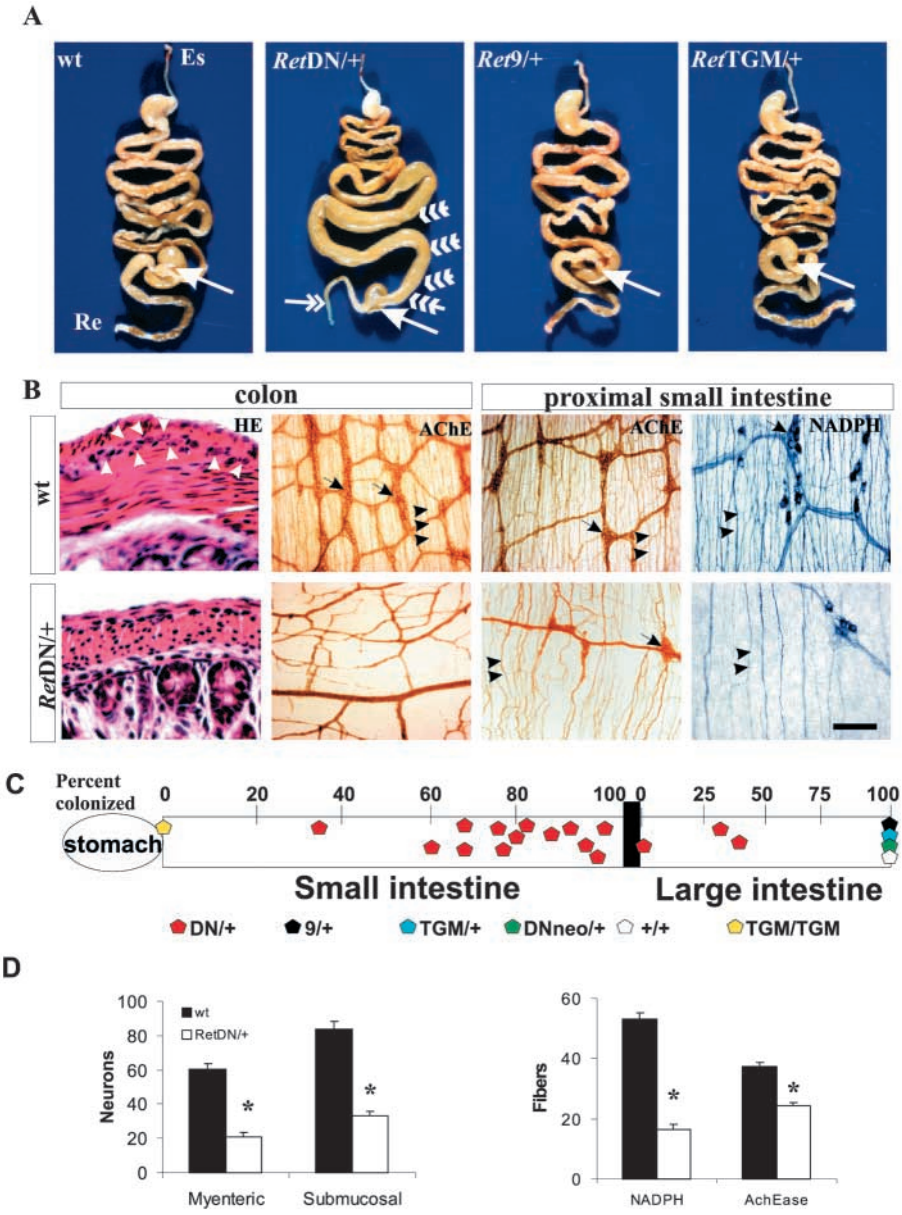

Fig. 2. Defects in enteric nervous system development in $Ret^{DN/+}$mice. (A) The intestines from a P21 $Ret^{DN/+}$ mouse with a contracted distal colon (double arrow) and a dilated distal small bowel (triple arrowheads). The intestines of wild-type (wt), $Ret^{9/+}$ and $Ret^{TGM/+}$ mice are normal (arrow, ileocecal junction; Es, esophagus; Re, rectum). (B) Intestinal aganglionosis and hypoganglionosis in P21 $Ret^{DN/+}$ mice. Hematoxylin and Eosin (HE) staining revealed the presence of neurons (arrowheads) in the muscularis externa of the colon in wild-type (wt) but not $Ret^{DN/+}$ mice. Acetylcholinesterase (AChE) staining demonstrated neuronal (black arrows) and nerve fiber (black arrowheads) loss in $Ret^{DN/+}$ colon (the brown fibers in the $Ret^{DN/+}$ colon are extrinsic innervations characteristic of HSCR). Both AChE- and nicotinamide adenine dinucleotide phosphate (NADPH)-stained $Ret^{DN/+}$ proximal small intestines display a reduced number of neurons (arrows) and nerve fibers (arrowheads), when compared with an identical region from wild-type mice. Scale bars: 100 μm (HE); 400 μm (AChE); 200 μm (NADPH). (C) The aganglionosis is fully penetrant but variable in $Ret^{DN/+}$ mice. The schematic shows the extent of aganglionosis determined by AChE staining in various $Ret^{DN/+}$ mice (each red mark represents one $Ret^{DN/+}$ mouse, n=16). The numbers correspond to the percentage of the respective intestinal segment (small or large intestine) successfully colonized by neurons. $Ret^{9/+}$ (n=7), $Ret^{DNneo/+}$ (n=3) and $Ret^{TGM/+}$ (n=3) intestines were normal, and $Ret^{TGM/TGM}$ (Ret null) had total intestinal aganglionosis. (D) Quantitative analysis of neuronal number and fiber density in the ENS of P21 wild-type and $Ret^{DN/+}$ mice demonstrated a dramatic reduction in the number of neurons and neuronal fiber density in the proximal small bowel (n=3, *=P<0.01, mean±s.e.m.).

NRTN-null mice, supporting the hypothesis that persistent Ret signaling is required for both the formation and proper function of SPG neurons.

The previous analysis of $Ret^{-/-}$ and $ARTN^{-/-}$ mice revealed that Ret signaling is also important for sympathetic neuron precursor migration and neuronal projections (Enomoto et al., 2001; Homma et al., 2003). In $Ret^{DN/+}$ mice, we found that, in contrast to in ARTN- and Ret-null mice, the SCG was properly located and had normal axonal projections to its targets (Fig. 3B). The sympathetic chain ganglia and their neurite outgrowths also developed normally. Thus, the $Ret^{DN/+}$ autonomic nervous system is differentially affected, with distinct morphological abnormalities in the parasympathetic, but not the sympathetic, nervous system.

Normal development of DRG sensory, spinal motor and midbrain dopaminergic neurons in $Ret^{DN/+}$ mice

GFL signaling has been implicated in the survival of midbrain dopaminergic, spinal motor and DRG sensory neurons in cell-culture and injury models (Beck et al., 1995; Bennett et al., 1998; Bowenkamp et al., 1995; Cacalano et al., 1998; Henderson et al., 1994; Lin et al., 1993; Molliver et al., 1997; Moore et al., 1996; Oppenheim et al., 1995; Oppenheim et al., 2000; Sanchez et al., 1996). Because these neurons continue to mature postnatally, and Ret-null mice die at birth, the importance of Ret activity for their proper postnatal function is unknown. We examined these neuronal populations in 3-week-old $Ret^{DN/+}$ mice, and found that they were morphologically normal. Thus, these neurons, unlike enteric and parasympathetic neurons, do not appear to be overtly sensitive to the diminished Ret activity caused by the *Ret*DN allele (see Fig. S1 in supplementary material).

Abnormal renal development in $Ret^{DN/+}$ mice

Mice with altered GDNF-GFRα1-Ret signaling have renal deficits with variable expressivity that range from cortical cysts to renal agenesis (de Graaff et al., 2001; Enomoto et al., 1998; Enomoto et al., 2001; Pichel et al., 1996; Sanchez et al., 1996;

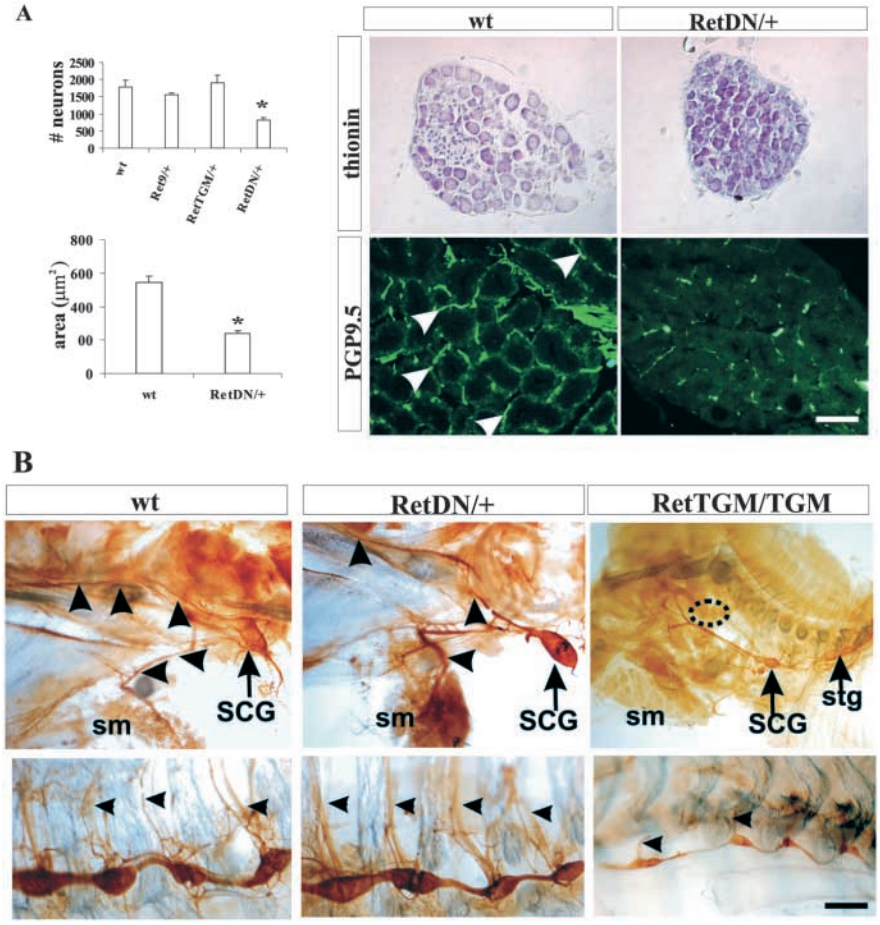

Fig. 3. Abnormal development of parasympathetic, but not sympathetic, ganglia in *Ret*$^{DN/+}$ mice. (A) The number, size and target organ innervation of sphenopalatine ganglia (SPG) parasympathetic neurons was decreased in *Ret*$^{DN/+}$ mice, when compared with wild-type (wt), *Ret*$^{9/+}$ and *Ret*$^{TGM/+}$ mutant animals. (Top left) Thionin-stained SPG neuron number per animal was decreased in *Ret*$^{DN/+}$ mice (P0). (Bottom left) The size of SPG neurons in *Ret*$^{DN/+}$ mice was 40-50% smaller than wild-type SPG neurons (n=3, *=P<0.01, mean± s.e.m.). (Top right) Thionin-stained *Ret*$^{DN/+}$ SPG neurons appear smaller than wild type (wt) (P21; scale bar: 50 μm). (Bottom right) The SPG target organ, the intraorbital harderian gland, showed a decrease of PGP9.5-stained nerve fibers in *Ret*$^{DN/+}$ mice compared with wild-type littermates where nerve fibers surround almost every acinus (arrowheads) Scale bar: 70 μm. (B) The sympathetic nervous system developed normally in *Ret*$^{DN/+}$ mice, as revealed by whole-mount tyrosine hydroxylase (TH) immunostaining (P0). (Top) The superior cervical ganglion (SCG) was normally located, and had normal projections to the eye (vertical arrowheads) and submandibular gland (sm, horizontal arrowheads) in *Ret*$^{DN/+}$ and wild-type (wt) mice (scale bar: 400 μm). (Bottom) The sympathetic chain ganglia and their neurite outgrowths (arrowheads) also appeared normal in *Ret*$^{DN/+}$ mice (scale bar: 300 μm). Abnormal development of the SCG (located more caudally near the stellate ganglion, stg; black circle indicates the expected SCG location), SCG projections (top right; scale bar: 800 μm), and sympathetic chain (bottom right; scale bar: 600 μm) in Ret-null mice (*Ret*$^{TGM/TGM}$) is shown for reference.

Schuchardt et al., 1996). These observations suggest that, as in other GDNF-dependent systems, renal development is sensitive to the level of effective GDNF signaling. The *Ret*$^{DN/+}$ kidneys were also variably affected, as animals were born either with both kidneys (57%), or with bilateral (18%) or unilateral renal agenesis (25%) (Fig. 4A). All kidneys in *Ret*$^{DN/+}$ mice were hypoplastic, with an approximate 50% decrease in glomeruli compared with that of their wild-type littermates (Fig. 4A). Unlike the distorted architecture of kidney rudiments observed in the few Ret-null mice that do not have complete renal agenesis, the hypoplastic *Ret*$^{DN/+}$ kidneys had histologically normal organization of the cortex and medulla at birth (n>9, data not shown). Among the animals surviving perinatal lethality, 70% (29/43) had both kidneys and 30% (14/43) had unilateral renal agenesis. Interestingly, 50% of *Ret*$^{DN/+}$ mice (6/12) at 3 to 4 weeks of age had renal tubular cysts and proteinaceous casts (Fig. 4A). The severity of the renal cystic anomalies ranged from a few cystic tubules to extensive parenchymal involvement. No renal abnormalities were noted in control mice (Ret$^{DNneo/+}$, n=5; Ret$^{TGM/+}$, n=10; Ret$^{9/+}$, n=15; Ret$^{+/+}$, n=20).

Defective spermatogenesis in *Ret*$^{DN/+}$ mice

A role for GFL signaling in testis biology was recently highlighted by the discoveries that mice overexpressing GDNF in the testes develop germ cell tumors, and that focal areas of abnormal spermatogenesis are present in GDNF heterozygotes (*Gdnf*$^{+/-}$) (Meng et al., 2000). Whether Ret mediates the GDNF effects on spermatogenesis is complicated by the death of *Ret*-null mice at birth (prior to the onset of spermatogenesis), and by the potential for Ret-independent GFL effects (Sariola and Saarma, 2003). The postnatal survival of the *Ret*$^{DN/+}$ mice allowed us to determine whether decreased Ret activity in these mice led to abnormal spermatogenesis. At 4 weeks of age, spermiogenesis had begun, and elongated spermatids were present in wild-type mice (Fig. 4B). However, the *Ret*$^{DN/+}$ seminiferous tubules showed marked degeneration, with multinucleated giant cells and cells with condensed nuclei. Furthermore, *Ret*$^{DN/+}$ testes showed maturation arrest, as evidenced by reduced numbers of round spermatids and the absence of elongated spermatids (Fig. 4C). The *Ret*$^{DN/+}$ ovaries were histologically normal at all ages examined (data not shown).

To further characterize the spermatogenesis defects in *Ret*$^{DN/+}$ mice, we first used TUNEL staining to examine apoptosis. Compared with wild-type mice at 4 weeks of age, the *Ret*$^{DN/+}$ seminiferous tubules contained large numbers of apoptotic cells that were primarily spermatocytes. The increased TUNEL staining was detected as early as postnatal day (P) 17 in *Ret*$^{DN/+}$ mice (Fig. 5B). Because abnormal

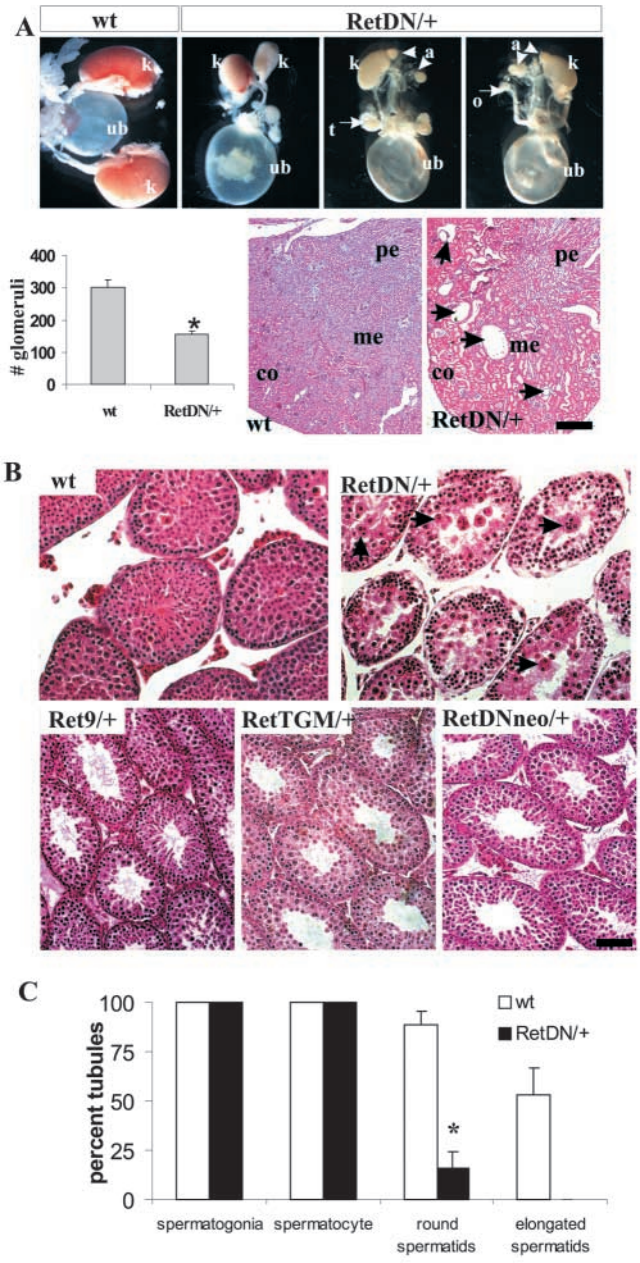

Fig. 4. Urogenital abnormalities in *Ret*$^{DN/+}$ mice. (A, top row). Compared with wild-type (wt) mice, *Ret*$^{DN/+}$ mice showed a spectrum of renal defects, including bilateral small kidneys and unilateral renal agenesis (k, kidney; a, adrenal; ub, urinary bladder, t, testis; o, ovary; adrenal gland, arrowhead). (A, bottom row) Bar graph shows the decreased total number of glomeruli in *Ret*$^{DN/+}$ kidney at birth (n=3 animals, 5 kidneys), when compared with wild-type litter mates (n=3 animals, 6 kidneys) (*=P<0.001, mean±s.e.m.). HE-stained sections show tubulocystic degeneration (arrows) in approximately 50% of 3- to 4-week-old *Ret*$^{DN/+}$ mice (6 out of 12) (co, cortex; me, medulla; pe, pelvis). Scale bar: 5 mm in top row; 600 μm in bottom row. (B) HE-stained sections show atrophic, degenerating seminiferous tubules with multinucleated giant cells (arrows) in *Ret*$^{DN/+}$ mice (P28). Wild-type (wt), *Ret*$^{9/+}$, *Ret*$^{TGM/+}$ and *Ret*$^{DNneo/+}$ mice show age-appropriate germ cell maturation. Scale bar: 100 μm for wild-type and *Ret*$^{DN/+}$ mice; 130 μm for *Ret*$^{9/+}$, *Ret*$^{TGM/+}$ and *Ret*$^{DNneo/+}$ mice. (C) At P28, a significant decrease in the percentage of *Ret*$^{DN/+}$ seminiferous tubules containing round spermatids is noted, and no tubules contain elongated spermatids (n=3 for each genotype, *=P<0.01, mean±s.e.m.).

spermatogenesis, by default, leads to apoptosis, we examined earlier time points for spermatogenesis defects. We first used a marker of early germ cells, germ cell nuclear antigen (GCNA), to determine whether the number of germ cells was decreased in *Ret*$^{DN/+}$ mice (Enders and May, 1994). We found

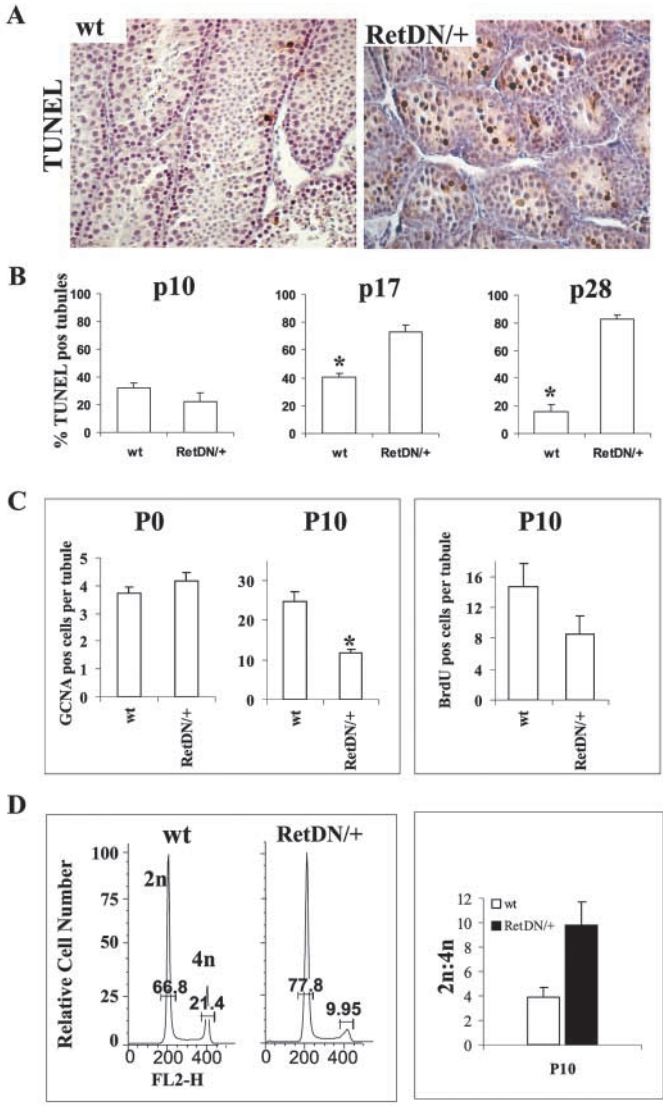

Fig. 5. Defective spermatogenesis in *Ret*$^{DN/+}$ mice is due to maturation delay and reduced germ cell number. (A) Representative picture depicting increased apoptosis by TUNEL staining (brown nuclei) in *Ret*$^{DN/+}$ seminiferous tubules at 3 to 4 weeks of age. (B) Increased apoptosis (TUNEL positive) in *Ret*$^{DN/+}$ seminiferous tubules was noted as early as P17 (n=3 for each time point, *=P<0.01, mean±s.e.m.). (C) *Ret*$^{DN/+}$ mice had a reduced number of germ cells by GCNA-immunostaining (left, n=3, *=P<0.01, mean±s.e.m.), and reduced cell proliferation (measured by BrdU incorporation, right, n=2, mean±s.d.), relative to wild-type (wt) mice at P10. Note the similar germ cell number between *Ret*$^{DN/+}$ and wild-type testes at birth. (D) Representative cell ploidy analysis of postnatal (P10) testes in *Ret*$^{DN/+}$ mice shows a higher 2n:4n ratio than in wild-type mice, indicating a delay in sperm maturation in *Ret*$^{DN/+}$mice. In the left panel, the 2n and 4n peaks are indicated, the numbers on the peaks represent the percentage of cells in each peak. The bar graph on right summarizes the ploidy results, which indicate a spermatogenesis defect at P10.

that, in newborn mice, the number of GCNA-stained germ cells was similar between wild-type and *Ret*$^{DN/+}$ testes (Fig. 5C). However, at P10, an age when spermatogonia (2n) typically differentiate into spermatocytes (4n) and then enter meiosis, the *Ret*$^{DN/+}$ testis had a marked decrease in total and proliferating germ cells per tubule, as assessed by GCNA and BrdU immunohistochemistry, respectively (Fig. 5C). We also tested whether there were alterations in the proportion of 2n and 4n germ cells in *Ret*$^{DN/+}$ testes, as this would reflect aberrant spermatogonial maturation. Using cell ploidy analysis, we found that the proportion of 4n cells was always lower in *Ret*$^{DN/+}$ testes, resulting in an increased 2n to 4n ratio at all time points (P10, P12 and P17) examined (Fig. 5D; data not shown). The above results suggest that a reduced number of precursors was available for meiosis, and explains the reduction in meiotic products (round and elongated spermatids) observed in P28 *Ret*$^{DN/+}$ mice (Fig. 4D). Hence, we conclude that Ret signaling is required in early spermatogenesis (between P0 and P10) to establish normal germ cell number and spermatogonial maturation.

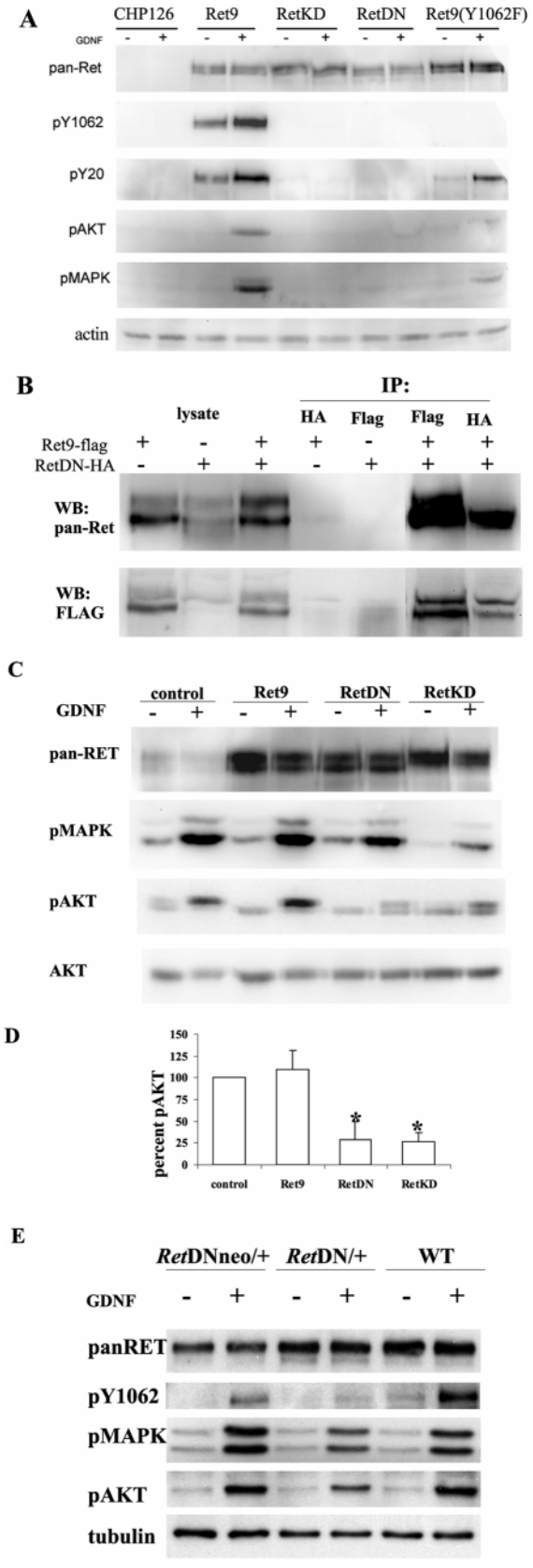

Mechanism of inhibition by the *Ret*DN allele

Mice with one wild-type Ret allele (*Ret*$^{+/-}$) are essentially normal, indicating that haploinsufficiency at the Ret locus cannot account for the severe deficits observed in *Ret*$^{DN/+}$ mice. We reasoned therefore that the Ret9(L985P, Y1062F) encoded by the RetDN allele acts in a dominant manner and inhibits the activity of the remaining wild-type Ret protein in the

Fig. 6. The RetDN mutant has decreased intrinsic kinase activity and inhibits wild-type Ret activity. (A) Western blots of extracts from CHP126 cells infected with the indicated Ret lentiviruses in the presence or absence of GDNF (25 ng/ml) were probed with the indicated antibodies. Wild-type Ret9 showed ligand-dependent autophosphorylation (pY20 and pY1062), and phosphorylation of downstream AKT and MAPK (pAKT and pMAPK, respectively), but RetDN and a kinase-inactive mutant with a K758M mutation (RetKD) lack these activities. (B) Immunoprecipitation studies demonstrated an interaction between RetDN and Ret9. Wild-type Ret9 (FLAG tagged) and RetDN (HA tagged) were co-expressed in 293T cells (which lack endogenous Ret). Lysates were immunoprecipitated with either FLAG- or HA-epitope specific antibodies, followed by western blotting (WB) using a pan-Ret antibody or a FLAG antibody to detect Ret9 and RetDN complexes. (C) RetDN inhibited ligand-dependent AKT phosphorylation. The human RET9 or RetDN were expressed in GDNF-responsive Neuro2Aα1 cells using lentivirus infection. The cells were grown in the presence or absence of GDNF, and western blots containing these cell lysates were probed with the indicated antibodies (pMAPK, phosphor-MAPK; pAKT, phosphor-AKT). Cells infected with RetDN, but not with wild-type Ret9, had markedly decreased levels of GDNF-dependent AKT phosphorylation, whereas MAPK phosphorylation was minimally affected. An antibody to AKT indicated equivalent total AKT levels in each sample. Control lanes represent lysates from cells infected with virus expressing only the Venus reporter. (D) Quantification of decreased AKT phosphorylation. The RetDN inhibition of AKT phosphorylation was quantified by normalizing the samples according to the total AKT levels and then comparing the GDNF-stimulated phospho-AKT levels. RetDN inhibited GDNF-mediated AKT phosphorylation by approximately 70% (n=3, *=P<0.01, mean±s.e.m.). (E) *Ret*DN inhibited endogenous mouse wild-type Ret activity in SCG neurons. Immunoblots of extracts from primary SCG neurons (cultured for 8 days) show decreased GDNF-dependent phosphorylation of Ret Y1062, AKT and MAPK in *Ret*$^{DN/+}$ mice, when compared with that of *Ret*$^{DNneo/+}$ and wild-type mice (WT). The blot was re-probed with tubulin antibody to ensure equal loading.

developing mouse. We performed a series of biochemical experiments in neuroblastoma cells to elucidate the mechanism of this dominant negative activity. First, CHP126 cells that do not express endogenous Ret were infected with lentiviruses expressing wild-type and/or mutant Ret molecules and lysates from these cells were analyzed in immunoblot experiments. We found that RetDN was expressed at normal levels, but had severely diminished ligand-dependent autophosphorylation and phosphorylation of the downstream AKT and MAPK signaling effectors (Fig. 6A). As mentioned above, it is unlikely that the decreased kinase activity of RetDN is responsible for the observed deficits in *Ret*$^{DN/+}$ mice, as one wild-type Ret allele is sufficient to guide normal development (Figs 2, 3, 4) (Enomoto et al., 2001; Schuchardt et al., 1994). Rather, the deficits are likely to arise from the formation of inactive heterodimers between wild-type Ret and mutant RetDN protein (i.e. dominant-negative inhibition). Support for this idea comes from co-immunoprecipitation experiments in 293T cells, using epitope-tagged versions of wild-type and mutant Ret. These experiments directly demonstrated an interaction between RetDN and wild-type Ret (Fig. 6B). We also investigated the ability of the RetDN to inhibit Ret signaling using the GDNF-responsive Neuro2Aα1cell line. We found that expression of RetDN inhibited ligand-dependent Ret phosphorylation and downstream signaling, with phosphorylation of AKT more affected than MAPK phosphorylation (Fig. 6C,D). Finally, we performed immunoblotting experiments to examine Ret activation in SCGs, which are GFL-responsive, from *Ret*$^{DN/+}$, *Ret*$^{DNneo/+}$ and wild-type animals. We found that the endogenous RetDN allele in *Ret*$^{DN/+}$ mice inhibits GDNF-dependent AKT and MAPK activation (Fig. 6E). Further investigation with phospho-specific antibodies directed at Ret Y1062 revealed decreased phosphorylation of this residue, a key residue for activation of the AKT/MAPK pathways. These observations demonstrate that RetDN acts as a dominant-negative receptor because its interaction with wild-type Ret inhibits ligand-dependent activation of downstream signaling pathways.

Discussion

Abnormal Ret activity has pleiotropic effects that range from tumor formation when Ret is too active to developmental abnormalities in humans and mice when Ret activity is reduced. Although Ret is clearly essential for normal development of the ENS, kidneys and autonomic nervous system, there are several crucial aspects of Ret function that remain poorly understood. First, although it is clear that Ret is required for proper embryonic development, the neonatal death of Ret-null mice has not allowed a direct assessment of its role in postnatal life. Instead, postnatal Ret functions, such as the maintenance of innervation have been surmised from the analysis of mice deficient for Ret ligands or co-receptors (NRTN, ARTN, PSPN, GFRα2, GFRα3, GFRα4) that survive after birth (Airaksinen and Saarma, 2002). The analyses of *Ret*$^{DN/+}$ mice in our study demonstrate that postnatal Ret function is essential for the normal formation of the enteric and parasympathetic nervous systems, the kidneys and spermatogenesis.

Second, it is puzzling why Ret mutations act dominantly to give rise to HSCR in humans, but Ret heterozygote mice have normal ENS development. The ENS defects in *Ret*$^{DN/+}$ mice suggest that intestinal aganglionosis is determined by the total amount of Ret signaling. For example, although an absence of Ret signaling results in complete intestinal aganglionosis in both humans and mice (Enomoto et al., 2001; Schuchardt et al., 1994; Shimotake et al., 2001; Solari et al., 2003), reduced Ret activity appears to be tolerated until a certain threshold is reached. Further decreases in activity then impact ENS precursor survival, proliferation and migration, and result in an aganglionic distal bowel. The aganglionosis in *Ret*$^{DN/+}$ mice is remarkably similar to long-segment HSCR caused by *RET* mutations in human populations, and makes these animals a useful model for studying HSCR pathobiology. For instance, we found profound hypoganglionosis in the proximal small bowel of *Ret*$^{DN/+}$ mice. Although it is not known whether small intestine hypoganglionosis occurs in children with HSCR because this bowel region is generally not evaluated, this finding provides a potential explanation for the persistent intestinal dysmotility observed in a large proportion of these patients even after resection of the aganglionic bowel (Tsuji et al., 1999).

Third, it is unknown whether the organs affected by Ret deficiency are differentially susceptible to levels of Ret activity. The surprisingly normal sympathetic nervous system but abnormally developed enteric and parasympathetic nervous systems and kidneys in the *Ret*$^{DN/+}$ mice suggest that the threshold of Ret signaling required for normal sympathetic nervous system development is different from that of other Ret-affected tissues. This 'sparing' effect may result from the preponderance of the Ret51 isoform in sympathetic neurons. As the *Ret*DN allele produces a mutant Ret9 isoform that may not interact with or inhibit Ret51 (Tsui-Pierchala et al., 2002), residual Ret51 activity in *Ret*$^{DN/+}$ SCG neurons may be sufficient for normal sympathetic nervous system development. Alternatively, the DN mutant could affect both Ret isoforms to some extent, and the remaining endogenous Ret activity (from both Ret9 and Ret51 isoforms) could be sufficient to support development of the sympathetic, but not the parasympathetic, nervous system.

Fourth, the role of Ret in kidney development after ureteric bud induction and early branching is unknown because Ret-null mice have renal agenesis and die at birth. The fact that *Ret*$^{DN/+}$ kidneys are hypoplastic but show normal renal architecture at birth only to degenerate over the next few weeks, suggests that Ret activity is required throughout nephrogenesis to maintain normal renal function. Hypoplastic kidneys due to decreased Ret signaling are also observed in transgenic mice that express Ret under the *Hox7b* promoter, and in Ret51 monoisomorphic mice that do not express the Ret9 isoform (Davies and Fisher, 2002; de Graaff et al., 2001; Lechner and Dressler, 1997; Srinivas et al., 1999). Because Ret9/Ret51 heterodimers are rare, and Ret9 is important for embryological development, the *Ret*$^{DN/+}$ kidney defects at birth are likely to be due to inhibition of the Ret9 isoform by the mutant *Ret*DN allele (de Graaff et al., 2001; Tsui-Pierchala et al., 2002). Expression studies suggest that the Ret51 isoform may be important in postnatal renal development and maintenance (Lee et al., 2002). Thus, the postnatal cystic abnormalities in *Ret*$^{DN/+}$ mice may be due to decreased Ret9 activity along with Ret51 haploinsufficiency. Interestingly, 40% of patients with renal agenesis harbor dominant *RET*

mutations predominantly in the tyrosine kinase domain (M. Skinner, personal communication), thus making the *Ret*$^{DN/+}$ mice a useful model of congenital human kidney disease.

Finally, while *Gdnf*$^{+/-}$ adult mice have abnormal spermatogenesis (Meng et al., 2000), the role of Ret activation in testes biology is uncertain because of the fact that spermatogenesis initiates well after birth. The survival of *Ret*$^{DN/+}$ mice beyond P0 allowed us to obtain definitive evidence that Ret signaling is required for the first wave of spermatogenesis. The *Ret*$^{DN/+}$ testes phenotype is much more severe than that of *Gdnf*$^{+/-}$ mice, because the first wave of spermatogenesis is distinctly abnormal, and this process occurs normally in *Gdnf*$^{+/-}$ mice. The defect in the first wave of spermatogenesis is apparent as early as P10, even before the onset of meiosis, and is consistent with the prepubertal expression of Ret in spermatogonia (Meng et al., 2000). These results suggest that Ret activity in *Ret*$^{DN/+}$ testes is even less than that of *Gdnf*$^{+/-}$ mice, and correlates well with abnormalities in the *Ret*$^{DN/+}$ ENS, the parasympathetic nervous system and the kidneys, which are also more severe than those observed in *Gdnf*$^{+/-}$ mice. Furthermore, it appears that certain events in spermatogenesis require different levels of Ret activity. For instance, small reductions in Ret activity in *Gdnf*$^{+/-}$ mice cause reduced spermatogonial cell renewal (Meng et al., 2000), whereas more severe reductions in Ret signaling in *Ret*$^{DN/+}$ animals prevent spermatogonial differentiation and cause apoptosis of spermatid precursors.

The phenotypic deficits observed in *Ret*$^{DN/+}$ mice are mediated by mutations L985P (kinase domain) and Y1062F (Shc docking site) of the *Ret*DN allele. Mutations in these Ret regions have been described in patients with HSCR (Geneste et al., 1999; Iwashita et al., 2001) and congenital kidney disease (M. Skinner, personal communication), and affect MAPK and/or AKT activation. Biochemical analysis from experiments in cell lines and primary SCG neurons expressing RetDN also show a reduction in AKT and MAPK activity. The preferential inhibition of AKT in vitro suggests that the developmental abnormalities observed in *Ret*$^{DN/+}$ mice are partly due to decreased signaling via the Ret(Y1062)-AKT pathway. This is consistent with several studies demonstrating that GFL-mediated activation of the PI3K-AKT pathway preferentially affects ENS and kidney development, and is crucial for neural crest precursor proliferation, survival and migration (Natarajan et al., 2002; Tang et al., 2002) (R.H., unpublished). However, it is possible that other Ret-stimulated signal transduction pathways, such as PLCγ, could also contribute to the phenotype observed in *Ret*$^{DN/+}$ mice. In this regard, it has been shown that mutations near the Ret(L985) in HSCR patients result in diminished PLCγ activity in vitro (Iwashita et al., 2001). We have not directly determined whether the abnormalities in *Ret*$^{DN/+}$ mice are due to mutations in the residues L985P or Y1062F, or both. However, the dominant-negative activity of this Ret mutant is likely to result from the RetL985P mutation, as the Ret9(Y1062F) mutant only affects phosphorylation of Ret at Y1062 (Encinas et al., 2004), Ret(L985P) alone is kinase deficient (data not shown), and recently generated mice that are heterozygous for a Ret9(Y1062F) allele (*Ret*$^{Y1062F/+}$) are viable and fertile (S.J., unpublished).

The analysis of *Ret*$^{DN/+}$ mice has enhanced our understanding of Ret function in postnatal development, provided novel insights into the function of GFL-Ret signaling complexes in vivo, and provided a valuable model to study how deficiencies in Ret signaling result in human diseases such as HSCR, and congenital kidney abnormalities. These mice will also be useful for investigating the importance of GFL-mediated Ret activation in adult animals. In particular, the ability to conditionally activate the RetDN inhibitory allele through Cre recombinase provides a method of assessing its role in maintaining specific neuronal populations, such as those affected in neurodegenerative diseases.

We thank Kelli Simburger, Shelly Audrain, Amber Nielson, Jennifer Armond, Tim Fahrner, Amanda Knoten, Tatiana Gorodinsky and Nina Panchenko for excellent technical assistance. We are grateful to Hideki Enomoto and Rex Hess for invaluable discussions, and Brian Tsui-Pierchala for Ret antibodies. This work was supported by NIH grants AG13730 and NS39358 (to J.M.) and T32CA09547-17 (to S.J.).

Supplementary material

Supplementary material for this article is available at
http://dev.biologists.org/cgi/content/full/131/21/5503/DC1

References

Airaksinen, M. S. and Saarma, M. (2002). The GDNF family: signalling, biological functions and therapeutic value. *Nat. Rev. Neurosci.* **3**, 383-394.

Baloh, R. H., Enomoto, H., Johnson, E. M., Jr and Milbrandt, J. (2000). The GDNF family ligands and receptors – implications for neural development. *Curr. Opin. Neurobiol.* **10**, 103-110.

Barrow, J. R. and Capecchi, M. R. (1996). Targeted disruption of the Hoxb-2 locus in mice interferes with expression of Hoxb-1 and Hoxb-4. *Development* **122**, 3817-3828.

Beck, K. D., Valverde, J., Alexi, T., Poulsen, K., Moffat, B., Vandlen, R. A., Rosenthal, A. and Hefti, F. (1995). Mesencephalic dopaminergic neurons protected by GDNF from axotomy-induced degeneration in the adult brain. *Nature* **373**, 339-341.

Bennett, D. L., Michael, G. J., Ramachandran, N., Munson, J. B., Averill, S., Yan, Q., McMahon, S. B. and Priestley, J. V. (1998). A distinct subgroup of small DRG cells express GDNF receptor components and GDNF is protective for these neurons after nerve injury. *J. Neurosci.* **18**, 3059-3072.

Bowenkamp, K. E., Hoffman, A. F., Gerhardt, G. A., Henry, M. A., Biddle, P. T., Hoffer, B. J. and Granholm, A.-C. E. (1995). Glial cell line-derived neurotrophic factor supports survival of injured midbrain dopaminergic neurons. *J. Comp. Neurol.* **355**, 479-489.

Cacalano, G., Farinas, I., Wang, L.-C., Hagler, K., Forgie, A., Moore, M., Armanini, M., Phillips, H., Ryan, A. M., Reichardt, L. F. et al. (1998). GFRα1 is an essential receptor component for GDNF in the developing nervous system and kidney. *Neuron* **21**, 53-62.

Clarke, P. G. and Oppenheim, R. W. (1995). Neuron death in vertebrate development: in vitro methods. *Methods Cell Biol.* **46**, 277-321.

Crowder, R. J., Enomoto, H., Yang, M., Johnson, E. M., Jr and Milbrandt, J. (2004). Dok-6, a novel p62 Dok family member, promotes Ret-mediated neurite outgrowth. *J. Biol. Chem.* **279**, 42072-42081.

Davies, J. A. and Fisher, C. E. (2002). Genes and proteins in renal development. *Exp. Nephrol.* **10**, 102-113.

de Graaff, E., Srinivas, S., Kilkenny, C., D'Agati, V., Mankoo, B. S., Costantini, F. and Pachnis, V. (2001). Differential activities of the RET tyrosine kinase receptor isoforms during mammalian embryogenesis. *Genes Dev.* **15**, 2433-2444.

Encinas, M., Crowder, R. J., Milbrandt, J. and Johnson, E. M., Jr (2004). Tyrosine 981, a novel ret autophosphorylation site, binds c-Src to mediate neuronal survival. *J. Biol. Chem.* **279**, 18262-18269.

Enders, G. C. and May, J. J., II (1994). Developmentally regulated expression of a mouse germ cell nuclear antigen examined from embryonic day 11 to adult in male and female mice. *Dev. Biol.* **163**, 331-340.

Enomoto, H., Araki, T., Jackman, A., Heuckeroth, R. O., Snider, W. D., Johnson, E. M., Jr and Milbrandt, J. (1998). GFR α1-deficient mice have deficits in the enteric nervous system and kidneys. *Neuron* **21**, 317-324.

Enomoto, H., Heuckeroth, R. O., Golden, J. P., Johnson, E. M. and Milbrandt, J. (2000). Development of cranial parasympathetic ganglia requires sequential actions of GDNF and neurturin. *Development* **127**, 4877-4889.

Enomoto, H., Crawford, P. A., Gorodinsky, A., Heuckeroth, R. O., Johnson, E. M., Jr and Milbrandt, J. (2001). RET signaling is essential for migration, axonal growth and axon guidance of developing sympathetic neurons. *Development* **128**, 3963-3974.

Geneste, O., Bidaud, C., de Vita, G., Hofstra, R. M., Tartare-Deckert, S., Buys, C. H., Lenoir, G. M., Santoro, M. and Billaud, M. (1999). Two distinct mutations of the RET receptor causing Hirschsprung's disease impair the binding of signalling effectors to a multifunctional docking site. *Hum. Mol. Genet.* **8**, 1989-1999.

Gianino, S., Grider, J. R., Cresswell, J., Enomoto, H. and Heuckeroth, R. O. (2003). GDNF availability determines enteric neuron number by controlling precursor proliferation. *Development* **130**, 2187-2198.

Henderson, C. E., Phillips, H. S., Pollock, R. A., Davies, A. M., Lemeulle, C., Armanini, M., Simpson, L. C., Moffet, B., Vandlen, R. A., Koliatsos, V. E. et al. (1994). GDNF: a potent survival factor for motoneurons present in peripheral nerve and muscle. *Science* **266**, 1062-1064.

Heuckeroth, R. O., Enomoto, H., Grider, J. R., Golden, J. P., Hanke, J. A., Jackman, A., Molliver, D. C., Bardgett, M. E., Snider, W. D., Johnson, E. M., Jr et al. (1999). Gene targeting reveals a critical role for neurturin in the development and maintenance of enteric, sensory, and parasympathetic neurons. *Neuron* **22**, 253-263.

Homma, S., Yaginuma, H., Vinsant, S., Seino, M., Kawata, M., Gould, T., Shimada, T., Kobayashi, N. and Oppenheim, R. W. (2003). Differential expression of the GDNF family receptors RET and GFRalpha1, 2, and 4 in subsets of motoneurons: a relationship between motoneuron birthdate and receptor expression. *J. Comp. Neurol.* **456**, 245-259.

Iwashita, T., Kurokawa, K., Qiao, S., Murakami, H., Asai, N., Kawai, K., Hashimoto, M., Watanabe, T., Ichihara, M. and Takahashi, M. (2001). Functional analysis of RET with Hirschsprung mutations affecting its kinase domain. *Gastroenterology* **121**, 24-33.

Lechner, M. S. and Dressler, G. R. (1997). The molecular basis of embryonic kidney development. *Mech. Dev.* **62**, 105-120.

Lee, D. C., Chan, K. W. and Chan, S. Y. (2002). RET receptor tyrosine kinase isoforms in kidney function and disease. *Oncogene* **21**, 5582-5592.

Lin, L.-F. H., Doherty, D. H., Lile, J. D., Bektesh, S. and Collins, F. (1993). GDNF: a glial cell line-derived neurotrophic factor for midbrain dopaminergic neurons. *Science* **260**, 1130-1132.

Lois, C., Hong, E. J., Pease, S., Brown, E. J. and Baltimore, D. (2002). Germline transmission and tissue-specific expression of transgenes delivered by lentiviral vectors. *Science* **295**, 868-872.

Majumdar, A., Vainio, S., Kispert, A., McMahon, J. and McMahon, A. P. (2003). Wnt11 and Ret/Gdnf pathways cooperate in regulating ureteric branching during metanephric kidney development. *Development* **130**, 3175-3185.

Meng, X., Lindahl, M., Hyvonen, M. E., Parvinen, M., de Rooij, D. G., Hess, M. W., Raatikainen-Ahokas, A., Sainio, K., Rauvala, H., Lakso, M. et al. (2000). Regulation of cell fate decision of undifferentiated spermatogonia by GDNF. *Science* **287**, 1489-1493.

Meyers, E. N., Lewandoski, M. and Martin, G. R. (1998). An Fgf8 mutant allelic series generated by Cre- and Flp-mediated recombination. *Nat. Genet.* **18**, 136-141.

Molliver, D. C., Wright, D. E., Leitner, M. L., Parsadanian, A. S., Doster, K., Wen, D., Yan, Q. and Snider, W. D. (1997). IB4-binding DRG neurons switch from NGF to GDNF dependence in early postnatal life. *Neuron* **19**, 849-861.

Moore, M. W., Klein, R. D., Farinas, I., Sauer, H., Armanini, M., Phillips, H., Reichart, L. F., Ryan, A. M., Carver-Moore, K. and Rosenthal, A. (1996). Renal and neuronal abnormalities in mice lacking GDNF. *Nature* **382**, 76-79.

Naldini, L., Blomer, U., Gage, F. H., Trono, D. and Verma, I. M. (1996). Efficient transfer, integration, and sustained long-term expression of the transgene in adult rat brains injected with a lentiviral vector. *Proc. Natl. Acad. Sci. USA* **93**, 11382-11388.

Natarajan, D., Marcos-Guitierrez, C., Pachnis, V. and de Graaff, E. (2002). Requirement of signalling by receptor tyrosine kinase RET for the directed migration of enteric nervous system progenitor cells during mammalian embryogenesis. *Development* **129**, 5151-5160.

Oppenheim, R. W., Houenou, L. J., Johnson, J. E., Lin, L.-F. H., Li, L., Lo, A. C., Newsome, A. L., Prevette, D. M. and Wang, S. (1995). Developing motor neurons rescued from programmed and axotomy-induced cell death by GDNF. *Nature* **373**, 344-346.

Oppenheim, R. W., Houenou, L. J., Parsadanian, A. S., Prevette, D., Snider, W. D. and Shen, L. (2000). Glial cell line-derived neurotrophic factor and developing mammalian motoneurons: regulation of programmed cell death among motoneuron subtypes. *J. Neurosci.* **20**, 5001-5011.

Pichel, J. G., Shen, L., Hui, S. Z., Granholm, A.-C., Drago, J., Grinberg, A., Lee, E. J., Huang, S. P., Saarma, M., Hoffer, B. J. et al. (1996). Defects in enteric innervation and kidney development in mice lacking GDNF. *Nature* **382**, 73-76.

Ponder, B. A. and Smith, D. (1996). The MEN II syndromes and the role of the ret proto-oncogene. *Adv. Cancer Res.* **70**, 179-222.

Rijli, F. M., Dolle, P., Fraulob, V., LeMeur, M. and Chambon, P. (1994). Insertion of a targeting construct in a Hoxd-10 allele can influence the control of Hoxd-9 expression. *Dev. Dyn.* **201**, 366-377.

Rossi, J., Luukko, K., Poteryaev, D., Laurikainen, A., Sun, Y. F., Laakso, T., Eerikainen, S., Tuominen, R., Lakso, M., Rauvala, H. et al. (1999). Retarded growth and deficits in the enteric and parasympathetic nervous system in mice lacking GFR alpha2, a functional neurturin receptor. *Neuron* **22**, 243-252.

Sanchez, M. P., Silos-Santiago, I., Frisen, J., He, B., Lira, S. A. and Barbacid, M. (1996). Renal agenesis and the absence of enteric neurons in mice lacking GDNF. *Nature* **382**, 70-73.

Sariola, H. and Saarma, M. (2003). Novel functions and signalling pathways for GDNF. *J. Cell Sci.* **116**, 3855-3862.

Schuchardt, A., D'Agati, V., Larsson-Blomberg, L., Costantini, F. and Pachnis, V. (1994). Defects in the kidney and enteric nervous system of mice lacking the tyrosine kinase receptor Ret. *Nature* **367**, 380-383.

Schuchardt, A., D'Agati, V., Pachnis, V. and Costantini, F. (1996). Renal agenesis and hypodysplasia in ret-k-mutant mice result from defects in ureteric bud development. *Development* **122**, 1919-1929.

Shimotake, T., Go, S., Inoue, K., Tomiyama, H. and Iwai, N. (2001). A homozygous missense mutation in the tyrosine kinase domain of the RET proto-oncogene in an infant with total intestinal aganglionosis. *Am. J. Gastroenterol.* **96**, 1286-1291.

Shimotake, T., Tomiyama, H., Aoi, S. and Iwai, N. (2003). Discrepancy between macroscopic and microscopic transitional zones in Hirschsprung[apos]s disease with reference to the type of RET/GDNF/SOX10 gene mutation. *J. Pediatr. Surg.* **38**, 698-701.

Solari, V., Ennis, S., Yoneda, A., Wong, L., Messineo, A., Hollwarth, M. E., Green, A. and Puri, P. (2003). Mutation analysis of the RET gene in total intestinal aganglionosis by wave DNA fragment analysis system. *J. Pediatr. Surg.* **38**, 497-501.

Srinivas, S., Wu, Z., Chen, C. M., D'Agati, V. and Costantini, F. (1999). Dominant effects of RET receptor misexpression and ligand-independent RET signaling on ureteric bud development. *Development* **126**, 1375-1386.

Svaren, J., Ehrig, T., Abdulkadir, S. A., Ehrengruber, M. U., Watson, M. A. and Milbrandt, J. (2000). EGR1 target genes in prostate carcinoma cells identified by microarray analysis. *J. Biol. Chem.* **275**, 38524-38531.

Tang, M. J., Cai, Y., Tsai, S. J., Wang, Y. K. and Dressler, G. R. (2002). Ureteric bud outgrowth in response to RET activation is mediated by phosphatidylinositol 3-kinase. *Dev. Biol.* **243**, 128-136.

Tsui-Pierchala, B. A., Ahrens, R. C., Crowder, R. J., Milbrandt, J. and Johnson, E. M., Jr (2002). The long and short isoforms of Ret function as independent signaling complexes. *J. Biol. Chem.* **277**, 34618-34625.

Tsuji, H., Spitz, L., Kiely, E. M., Drake, D. P. and Pierro, A. (1999). Management and long-term follow-up of infants with total colonic aganglionosis. *J. Pediatr. Surg.* **34**, 158-161.